Catalysis Today 142 (2009) 252–257

Contents lists available at ScienceDirect

Catalysis Today

journal homepage: www.elsevier.com/locate/cattod

Ethanol reforming and partial oxidation with Cu/Nb_2O_5 catalyst

Carlos E.M. Guarido [a], Deborah V. Cesar [a], Mariana M.V.M. Souza [a,b], Martin Schmal [a,*]

[a] NUCAT/PEQ/COPPE - Federal University of Rio de Janeiro/UFRJ, Centro de Tecnologia, Bloco G, sala 128, CEP 21945-970, Rio de Janeiro/RJ, Brazil
[b] Escola de Química - UFRJ, Centro de Tecnologia, Bloco E, sala 206, CEP 21941-909, Rio de Janeiro/RJ, Brazil

ARTICLE INFO

Article history:
Available online 24 September 2008

Keywords:
Ethanol
Reforming
Hydrogen
Copper
Niobia

ABSTRACT

Ethanol reforming and partial oxidation were studied on Cu/Nb_2O_5 and Ni/Al_2O_3 catalysts. Compared to the Ni/Al_2O_3 catalyst, the Cu/Nb_2O_5 catalyst presents conversion as high as Ni/Al_2O_3 catalyst, however, for the same level of formation of hydrogen it occurs at much lower temperature on the Cu/Nb_2O_5 catalyst, 200 °C lower than for the Ni/Al_2O_3 catalyst, with remarkable little formation of CO, which can be attributed to the strong interaction between copper and niobia. Temperature-programmed desorption (TPD-ethanol) and surface reactions (TPSR) of partial oxidation of ethanol showed formation of ethylene, acetaldehyde, ethane and mainly H_2 and CO_2 besides little methane. DRIFTS results are in accordance with TPD analysis and the formation of acetate species at room temperature suggests reactivity of the surface and its oxidative dehydrogenation capacity. The adsorption of ethanol gives rise to ethoxide species, which form acetate and acetaldehyde that can be oxidized to CO_2 via carbonate. A comparison with reported results for Cu/Al_2O_3 this catalyst is promising, yielding high level of H_2 with little CO production during reforming and partial oxidation reaction. The maximum H_2 formation for the partial oxidation of ethanol was 41% at ratio (O_2/Et) 0.8, increasing to 50% at ratio 1.5. The H_2/CO is around 10 for the partial oxidation and 7 for steam reforming, which is excellent, compared to the Ni/Al_2O_3 catalyst with a factor 4–8 lower.

1. Introduction

Nowadays, increasing attention is being paid to pollution-related environmental and public health problems. Particularly, as one of the major contributor to the atmospheric pollution, the automotive section had to work hard on pollution control. Both catalytic converters on gasoline-fueled engines and filters for particulates on diesel-fueled engines were implemented.

The next step, to overpass the forthcoming regulations on CO_2 emissions according to the Kyoto's Protocol (in Europe, 8% reduction compared to the 1990s emissions by 2008–2012, EUA 7%), requires the development of both new engines and alternative fuels [1].

Bio-ethanol, presented as an environmentally fuel (renewable, CO_2 neutral, non-toxic), is used in catalytic steam reforming reaction or partial oxidation for H_2 onboard production.

Thermodynamically these reactions are possible; however, the great challenge is to find out catalysts with high stability, active and mainly selective for hydrogen. In addition, these catalysts must be resistant to coke formation. The interest for hydrogen production from ethanol has increased in the last years, and there are some new catalysts with different metals and supports [2–5].

Auprêtre et al. [6] studied catalysts for reforming of ethanol with high selectivity to CO_2 (minimum CO formation) with a series of metals (Rh, Pt, Pd, Ru, Ni, Cu, Zn, Fe) and different supports (Al_2O_3, 12% $CeO_2–Al_2O_3$, CeO_2, $CeO_2–ZrO_2$, ZrO_2). Ni and Rh supported on alumina were the most promising catalysts in terms of activity and selectivity and the activity depends directly on the decreasing mobility of OH groups at the surface. The activity follows in decreasing order: $Rh \geq Ni > Pd > Pt > Cu = Zn > Ru = Fe$.

Alberton et al. [7] studied steam reforming over Ni/Al_2O_3 catalysts varying the Ni content (8 and 16%) and the support (α and γ/alumina) and analyzed the effect of activation on the activity and carbon formation. As reported the activation method affected the stability and the nature of carbon influenced the stability.

Cavallaro and Freni [8] studied the ethanol reforming with mixed oxide catalyst $CuO/ZnO/Al_2O_3$, showing that the main products CO, CO_2 and H_2 are formed above 350 °C. Cooper supported on alumina was studied in the ethanol reforming, showing that copper promoted a rapid dehydrogenation of ethanol to acetic aldehyde, while nickel favored the rupture of carbon–carbon bonds of ethanol, with formation of methane and carbon monoxide [9].

Niobium oxide is a reducible material and presents strong metal support interaction, depending of the reduction temperature

---

[*] Corresponding author. Fax: +55 21 25628360.
E-mail address: schmal@peq.coppe.ufrj.br (M. Schmal).

0920-5861/$ – see front matter © 2008 Elsevier B.V. All rights reserved.
doi:10.1016/j.cattod.2008.08.030

[10,11], which is important for oxidation and hydrogenation reactions, besides redox properties, and has not been studied for the ethanol reforming or partial oxidation of ethanol. These properties may favor the partial oxidation and even the reforming of ethanol in the presence of a metal.

Therefore, the main objective of this paper is to study Cu supported on niobia for ethanol reforming and partial oxidation and determine the surface properties using temperature-programmed desorption (TPD) and in situ diffuse reflectance infrared Fourier transform spectroscopy (DRIFTS) analysis. The Ni/Al_2O_3 catalyst was used as reference in the catalytic tests.

2. Experimental

2.1. Catalyst preparation

Nb_2O_5 (41 m^2/g) (calcination of niobic acid – $Nb_2O_5 \cdot nH_2O$ – CBMM at 500 °C for 2 h) was impregnated with a solution of $Cu(NO_3)_2 \cdot 3H_2O$ (Merk), at 80 °C under vacuum until complete evaporation. The sample was dried at 100 °C for 18 h and then calcined at 550 °C for 2 h, under flowing air (60 mL/min). The theoretical content of CuO was 15 wt.%. The real content was 14.9% in good agreement with the theoretical value.

The Ni/Al_2O_3 catalyst was prepared by impregnation, using $Ni(NO_3)_2$ as precursor in a rotavapor, under stirring and vacuum at 80 °C until complete evaporation of the solution. Then the sample was dried at 100 °C for 18 h and calcined at 500 °C. The nickel content was 14 wt.%, equivalent to that reported in the literature [7]. The surface area was 198 m^2/g and the real content of nickel was 13.9%, in good agreement with the theoretical value.

2.2. Catalyst characterization

Temperature-programmed reduction (TPR) was performed using a conventional equipment with a thermal conductive detector (TCD). 10 mg of active phase (copper) was inserted into a quartz reactor and dehydrated at 200 °C for 2 h in a flow of pure argon. TPR was performed with a reductive mixture of 1.74%H_2/Ar (30 mL/min), and the temperature was raised up to 900 °C at 10 °C/min.

Temperature-programmed desorption was performed to investigate the surface active sites and adsorption and reaction properties with increasing temperature, using a dynamic mode apparatus. The amount of catalyst was 50 mg and a He feed flow rate of 40 mL/min. The effluent gas composition was monitored on-line by a quadrupole mass spectrometer (Dycor MA100M, Ametek).

Temperature-programmed surface reactions (TPSR) measurements were carried out in the same unit with a quadrupole mass spectrometer (Balzers Prisma, QMS 200). The sample was saturated with ethanol at 25 °C, followed by flowing 5% O_2/He (40 mL/min) at 20 °C/min up to 400 °C. The signal intensities of masses were monitored continuously. Quantifications were carried through calibration of each component and expressed in mole%.

DRIFTS experiments were performed in a Thermo Nicolet Nexus 470 spectrometer equipped with an MCT-A detector (cooled with liquid nitrogen), and a high-temperature cell (Thermo Spectra-Tech) fitted with ZnSe windows. Spectra were acquired at a resolution of 4 cm^{-1} typically averaging 64 scans. First, the sample was reduced under H_2 flow (10%H_2/He) at 30 mL/min and at 500 °C for 1 h, degassed with He flow and cooled to RT. Then ethanol (0 °C) was fed into the cell with He flow through the saturator for 30 min and the spectrum recorded. The chamber was closed with ethanol, recorded and then cleaned with He flow to remove reversible ethanol. Then, under He flow and heating at different temperatures, spectra were recorded at 100, 200, 300 and 350 °C. The spectrum of the sample after reduction was used as reference.

2.3. Catalytic tests

Reforming and partial oxidation of ethanol were performed in a flow microreactor at 1 atm and temperature varying between 200 and 700 °C, using 100 mg of catalyst and He flow passing through a saturator at 50 mL/min. The water/ethanol flow rate was 40 mL/min and the water/ethanol molar ratio were 1.5 and 3. The flow rate of oxygen/ethanol was 40 mL/min and the oxygen/ethanol ratio was 0.8 and 1.5. Products were analyzed on-line using a VARIAN CP-3800 chromatography, equipped with a column PoraPLOT Q and two detectors, thermal conductivity (TCD) and ionization flame (FID). The catalyst was first reduced in situ with a mixture of 10% H_2 in He at 44 mL/min and at 500 °C for 1 h.

3. Results and discussion

3.1. Catalyst characterization

The reducibility of the Cu/Nb_2O_5 was studied by TPR under H_2/Ar flow in the range from 25 to 900 °C. The H_2 response as a function of temperature is presented in Fig. 1. The Cu/Nb_2O_5 presents one main peak at 420 °C, which corresponds to the reduction of Cu^{2+} to Cu^0, with a small shoulder around 300 °C attributed to the reduction of unreduced Cu^{2+} to Cu^{1+}. Calculations showed that the H_2 consumption was 144 $\mu mol/g_{cat}$, which corresponds exactly to the theoretical consumption for the reduction of $Cu^{2+} \rightarrow Cu^0$, indicating a complete reduction of copper oxide.

The TPR profile of nickel (not shown) presented two reduction peaks at 420 and 852 °C, which corresponds to the reduction of NiO to metallic Ni^0 and of the $NiAl_2O_4$ aluminate phase, respectively. The H_2 consumption was 1.50 mmol/g, while the needed consumption to metallic Ni^0 was 2.63 mmol/g, corresponding to a reduction degree of 57%.

The literature is scarce on Cu/Nb_2O_5 characterizations and consequently the results compared with Cu/Al_2O_3 present similarities. In particular the TPR results on alumina supported copper reported by Jiang et al. [12] and Xiaoyuan et al. [13] showed that the reduction occurs around 400 °C, for Cu contents of the same order and complete reduction of copper.

Figs. 2 and 3 present the desorption profiles during TPD of ethanol for Cu/Nb_2O_5 and Ni/Al_2O_3 catalysts, respectively. At 170 °C ethanol desorption is possibly due to weak interaction

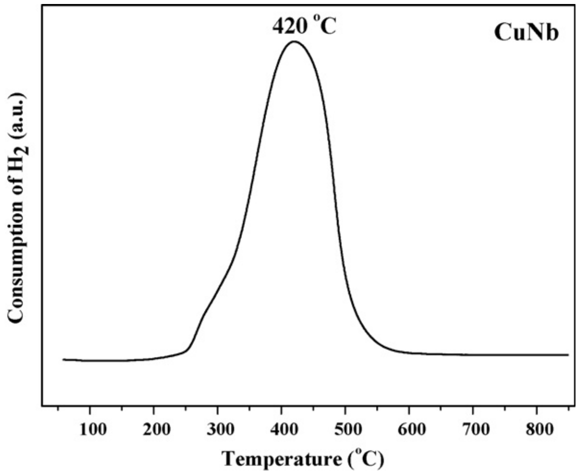

Fig. 1. TPR profile of Cu/Nb_2O_5 catalyst.

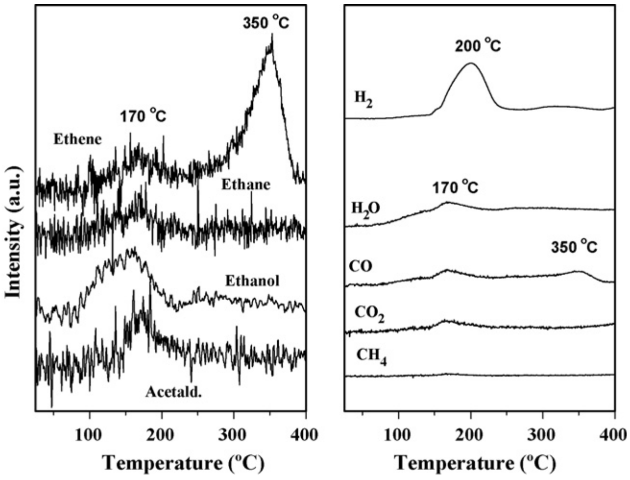

Fig. 2. TPD profiles of ethanol on Cu/Nb_2O_5 catalyst.

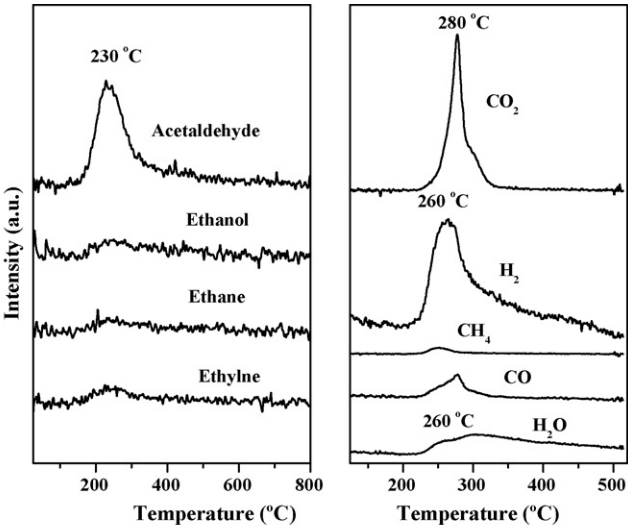

Fig. 4. TPSR analysis after ethanol adsorption and flowing $5\%O_2/He$.

between the remaining multilayers and the catalytic surface. Still at 170 °C occurred the dehydrogenation and dehydration of ethanol to form acetaldehyde and ethene, respectively, and formation of ethane. Besides, there is a little formation of CO and CO_2, which can be attributed to the WGSR at low temperature and due to the low water/ethanol ratio. Therefore, the prevailing reactions are:

$$C_2H_5OH \rightarrow CH_3CHO + H_2 \quad (1)$$

$$C_2H_5OH \rightarrow C_2H_4 + H_2O \quad (2)$$

$$C_2H_5OH + H_2 \rightarrow C_2H_6 + H_2O \quad (3)$$

At higher temperatures it was shown the presence of CO and H_2 due to the reforming of ethanol:

$$C_2H_5OH + H_2O \rightarrow 2CO + 4H_2 \quad (4)$$

At 350 °C one observed the formation of ethene due to reaction 2. In this case the formation of methane is low.

TPSR analysis (Fig. 4) shows the profiles after adsorption of ethanol passing $5\%O_2/He$ flow with increasing temperature on Cu/Nb_2O_5 catalyst. One can observe formation of acetaldehyde at 230 °C with very small production of ethylene and ethane. However, during programming oxidation there are formation of H_2 and CO_2 at 260 and 280 °C, respectively due to partial oxidation reaction of ethanol. Besides, there are little formation of CO, CH_4 and water around these temperatures. Compared with the TPD profiles of ethanol these profiles are very similar, that means, decomposition of ethanol is not the limiting step of oxidation. Since the CO_2 peak is lower than the temperature necessary for desorption or decomposition of ethanol it may be suggested that intermediate species at the surface are formed at lower temperatures. The formation of CO and CO_2 are mainly observed on niobia (not shown) and the addition of a metal was important for the formation of H_2.

3.2. Catalytic tests

Fig. 5 displays the conversion of steam reforming of ethanol and the molar fraction with temperature for H_2O/ethanol molar ratios of 1.5 and 3. As shown, the conversion of ethanol is complete around 400 °C. The main product at 200 °C is

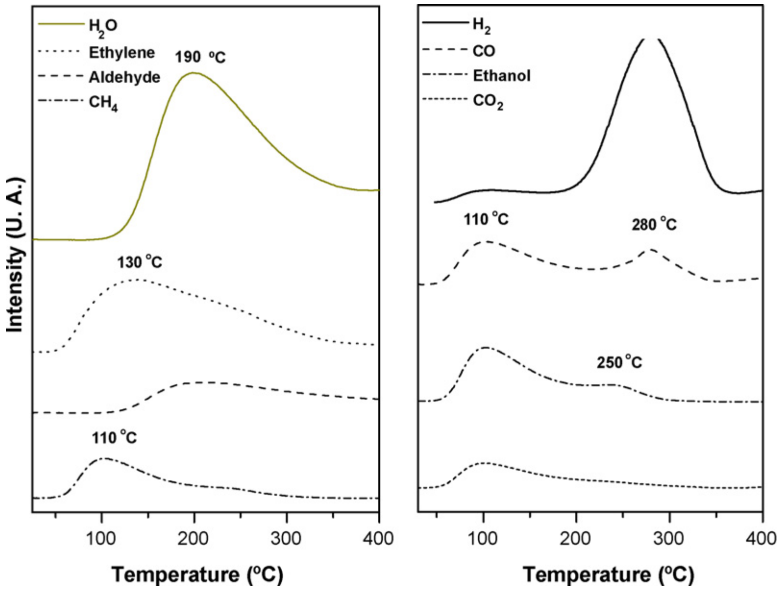

Fig. 3. TPD profiles of ethanol on Ni/Al_2O_3 catalyst.

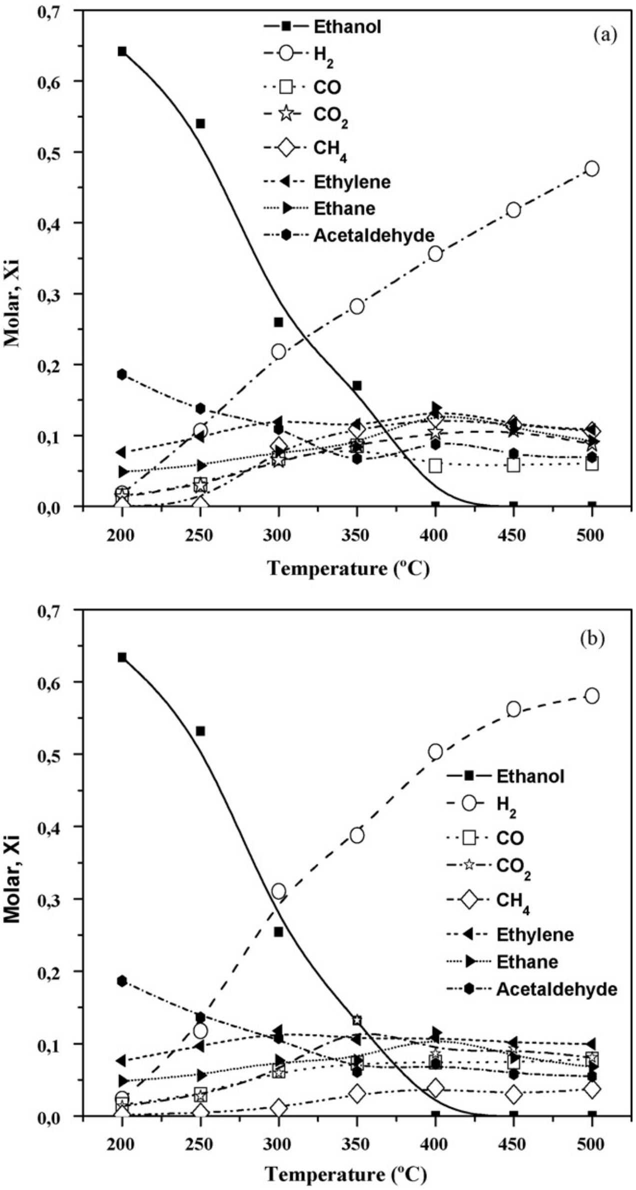

Fig. 5. Molar fractions as function of the temperature during steam reforming of ethanol using water/ethanol ratio of 1.5 (a) and 3 (b).

acetaldehyde due to the dehydrogenation of ethanol. With increasing temperature and for both ratios the acetaldehyde decreases drastically up to 350 °C, increasing up to 400 °C and than decreases. It agrees with the TPD results where the maximum peak of acetaldehyde was observed around 170 °C. The molar fraction of ethene and ethane are 12% at 300 °C and 14% at 400 °C, respectively, and according reactions (2) and (3), very similar for both ratios. Methane formation was observed due to the decomposition of ethanol and acetaldehyde, while CO_2 by steam reforming at a ratio of 1.5 up to 350 °C and due to reforming and shift reaction between 350 and 400 °C.

$$C_2H_5OH \rightarrow CO + CH_4 + H_2 \quad (5)$$

$$CH_3CHO \rightarrow CH_4 + CO \quad (6)$$

On the other hand, carbon monoxide is produced by reforming and decomposition of ethanol up to 300 °C for both ratios. However, between 350 and 400 °C and a ratio 1.5 the shift reaction is favored, but after 400 °C the carbon monoxide reforming prevails.

For a water/ethanol ratio of 3 the carbon monoxide increases up to 500 °C due to the reforming reaction. Hydrogen is produced soon after 300 °C either for the ratio 1.5 and 3, mainly due to the reforming of ethanol and shift reaction. The maximum production of H_2 was 58% around 500 °C, for water/ethanol ratio of 3.

For comparison we plotted the selectivity as function of the temperature for the Cu/Nb_2O_5 and Ni/Al_2O_3 catalysts, as displayed in Fig. 6 using the same H_2O/ethanol ratio 1.5. Similar behavior was observed for the ratio 3.0. Notice that there are distinguished results. The H_2 selectivity for Cu/Nb_2O_5 and Ni/Al_2O_3 catalyst reached 50%, for the same conversion (90% conversion) but at different temperatures, respectively 380 and 600 °C, for the Cu/Nb_2O_5 and Ni/Al_2O_3 catalyst, that means, a difference of 220 °C. Moreover, as observed from Fig. 6, the CO formation is much lower for the Cu/Nb_2O_5 than for the Ni/Al_2O_3 catalyst, for the same conversion (50%). The CO selectivity was 0.033 (400 °C) for Cu/Nb_2O_5 and 0.170 (600 °C) for Ni/Al_2O_3 catalysts, which is a factor of 3. The CO/CO_2 ratio is also quite different, i.e., 0.538 and 1.134 for Cu/Nb_2O_5 the Ni/Al_2O_3 catalysts, respectively, representing a factor of 2.1. Fig. 6b shows also that depending on the temperature the Ni/Al_2O_3 catalyst produces different products, in particular acetaldehyde and ethylene or methane at lower temperatures, which is not detectable for the Cu/Nb_2O_5 catalyst. These products decrease with increasing temperature above 500 °C, while for the

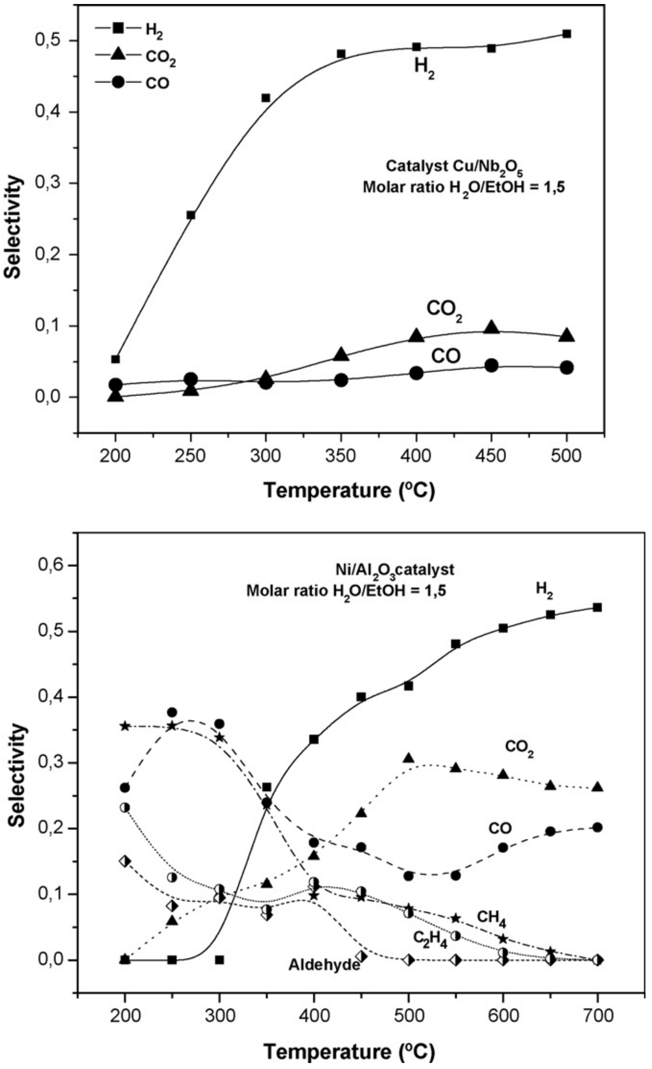

Fig. 6. Selectivity as function of the temperature during steam reforming of ethanol using water/ethanol ratio of 1.5 for Cu/Nb_2O_5 (a) and Ni/Al_2O_3 (b) catalysts.

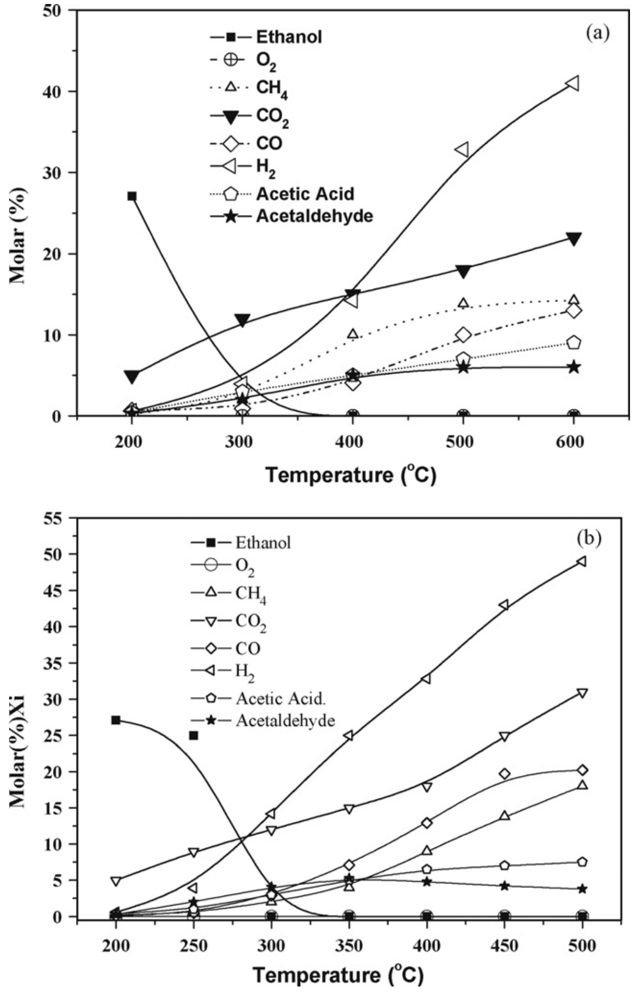

Fig. 7. Molar fractions as function of the temperature during partial oxidation of ethanol on Cu/Nb_2O_5 catalyst using O_2/ethanol ratio of 0.8 (a) and 1.5 (b).

Cu/Nb_2O_5 catalyst even for lower temperatures, the formation of these products is very low. The H_2/CO is around 7–8 at 500 °C, which is excellent. The H_2/CO is around 1.6 at 700 °C for the Ni/Al_2O_3 catalyst, a factor of approximately 4–5.

Comparing TPD results of the Cu/Nb_2O_5 and Ni/Al_2O_3 catalysts, as displayed in Figs. 2 and 3, one can observe distinguish profiles. Noteworthy are the profiles of acetaldehyde, CO and water, displaying lower signals on Cu/Nb_2O_5 than on Ni/Al_2O_3 catalysts, which indicate de different mechanisms. While on Ni/Al_2O_3 catalyst prevails the dehydration and decomposition of ethanol, on Cu/Nb_2O_5 one can observe prevailing reaction of decomposition (5) accompanied with the shift reaction.

$$CO + H_2O \rightarrow CO_2 + H_2 \qquad (7)$$

Fig. 7 presents the molar fraction distribution of the different products for the partial oxidation of ethanol on Cu/Nb_2O_5 catalyst with temperature and different ratios O_2/ethanol 0.8 and 1.5. Ethanol is completely converted around 300 °C and oxygen around 200 °C. The main products are CO and CO_2, but with increasing temperature acetic acid and acetaldehyde are produced. CO_2 is the principal product due to the oxidation of ethanol. CO is observed due to the decomposition and oxidation of ethanol. Hydrogen is produced at 200 °C for both ratios, attributed to the decomposition and oxidation of ethanol with increasing temperature. The maximum H_2 content was 41% at ratio 0.8, increasing to 50% at ratio 1.5. The H_2/CO is around 10, which is excellent. The H_2/CO is around 1.6 for the Ni/Al_2O_3 catalyst.

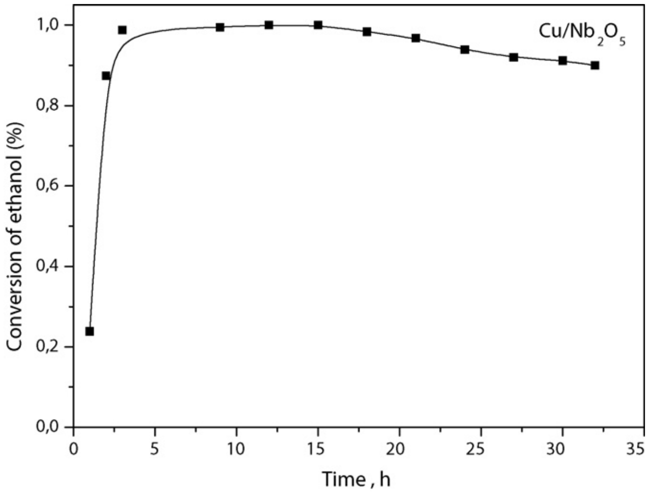

Fig. 8. Deactivation with time on stream for steam reforming of ethanol using water/ethanol ratio of 1.5 for Cu/Nb_2O_5 catalyst.

3.3. Deactivation tests

The conversion for Cu/Nb_2O_5 catalyst is presented as function of time, as shown in Fig. 8. Both (for Ni/Al_2O_3 not shown) are relatively very stable up to 30 h, however, the Cu/Nb_2O_5 is more stable with time on stream decreasing less then 5%, while the Ni/Al_2O_3 decreases twofold. An initial activation was observed on both catalysts, which is attributed to the H_2 formation during the first 2–5 h. It helps to reduce CuO or NiO into metallic Cu^0, or Ni^0, which explains the induction time during the reaction. In accordance with our previous report [7] the type of carbon formed indicate the formation filamentous carbon that may increase the activity, however the encapsulated coke promote the deactivation. In the present case the deactivation is slow and is mainly attributed to the carbon deposition, blocking the pores.

3.4. DRIFTS

Fig. 9 displays the DRIFT spectra after adsorption of ethanol on Cu/Nb_2O_5 under flow and closed conditions with different times.

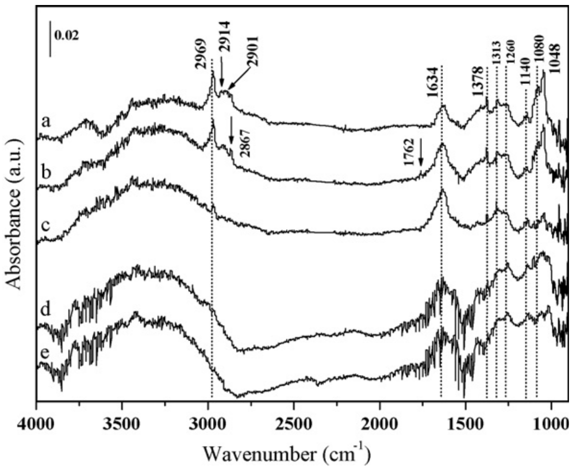

Fig. 9. DRIFTS spectra after adsorption of ethanol and desorption at different temperatures on Cu/Nb_2O_5. (a) Flow of EtOH after 30 min at 30 °C, (b) closed chamber for 15 min, (c) after He flow 15 min, (d) closed chamber at 100 °C for 5 min, (e) He flow at 100 °C for 5 min.

The most intense bands after ethanol adsorption were observed at 2969 cm^{-1} (υ_a CH_3), 2914 cm^{-1} (υ_a CH_2), 2901 cm^{-1} (υ_s CH_2), 2867 cm^{-1} (υ_s CH_3), 1313 cm^{-1} (δ_s CH_3) and around 1400 cm^{-1} (δ_a CH_3, CH_2) due to surface ethoxide species. At 1080 and 1047 cm^{-1} ethoxide species are adsorbed on the surface in bidentate form [14]. In accordance with the literature (Mavrikakis and Barteau [14]), primary alcohols adsorb on the metallic oxide surfaces as alkoxide from the scission of the O–H bond. The band at 1634 cm^{-1} corresponds to adsorbed water, while bands at 1140, 1378 and 1260 cm^{-1} indicate the presence of acetate species (COC) adsorbed on the oxygen of the niobia lattice, which remains very stable with the temperature. After closing the chamber slight modification was observed in the spectrum; one can observe a small band at 1762 cm^{-1} that indicates acetaldehyde in the gas phase (δ C=O), which disappears after He flow. Heating at 100 °C the band intensities decrease and acetate species are still present.

The results show that ethanol adsorbs as ethoxide and is oxidized to acetate species at room temperature, probably due to the redox property of niobia. The band intensities decrease with increasing temperature. The ethoxide species are decomposed at about 200 °C. It is in accordance with formation of CO, CO_2 and H_2 during TPD of ethanol, also attributed to these ethoxide species. Our TPD results confirm the decomposition of ethanol at 170 °C and above 345 °C, which is attributed to the oxidative dehydrogenation of adsorbed ethanol, and is in accordance with DRIFTS results, showing the formation of acetaldehyde at 1700 cm^{-1}. Yee et al. [15,16] suggested that these acetaldehyde species may decompose into CH_4 and CO or into carbonates, which are then oxidized with the formation of CO_2. Based on these results one can suggest a reaction path, which follows:

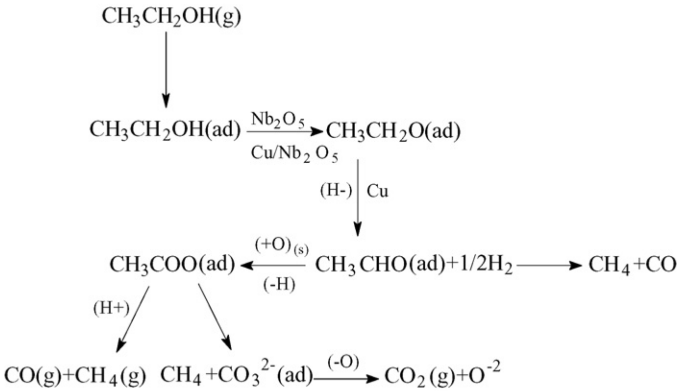

4. Conclusions

The desorption profiles of ethanol for Cu/Nb_2O_5 catalyst showed dehydrogenation and dehydration of ethanol to form acetaldehyde and the ethene, respectively, at 170 °C. At higher temperatures it was shown the presence of CO and H_2 due to the decomposition and reforming of ethanol. In this case the formation of methane was insignificant.

The Cu/Nb_2O_5 catalyst presents as high conversion as Ni/Al_2O_3 catalyst for steam reforming and partial oxidation of ethanol, however, for the formation of hydrogen at the same level it occurs at much lower temperature, 200 °C lower than for the Ni/Al_2O_3 catalyst and noteworthy is the little formation of CO on the Cu/Nb_2O_5 catalyst compared to the Ni/Al_2O_3 catalyst, which can be attributed to the strong interaction between the metal and the support.

DRIFTS results are in accordance with TPD analysis and the formation of acetate at room temperature suggests reactivity of the surface and its oxidative dehydrogenation capacity.

On the basis of the results one can propose a mechanism for steam reforming of ethanol on copper/niobia catalyst. The adsorption of ethanol gives rise to ethoxide species, which form acetate and acetaldehyde that can be oxidized to CO_2 via carbonate species with increasing temperature.

References

[1] A.S. Dagoumas, G.K. Papagiannis, P.S. Dokopoulos, Energy Policy 34 (2006) 26.
[2] D.K. Liguras, D.I. Kondarides, X.E. Verykios, Appl. Catal. B: Environ. 43 (2003) 345.
[3] A.N. Fatsikostas, D.I. Kondarides, X.E. Verykios, Catal. Today 75 (2002) 145.
[4] D.K. Liguras, K. Goundani, X.E. Verykios, Int. J. Hydrogen Energy 29 (2004) 419.
[5] S. Cavallaro, V. Chiodo, S. Freni, N. Mondello, F. Frusteri, Appl. Catal. A: Gen. 249 (2003) 119.
[6] F. Auprêtre, C. Descorme, D. Duprez, Catal. Commun. 3 (2002) 263.
[7] A.L. Alberton, M.M.V.M. Souza, M. Schmal, Catal. Today 123 (2007) 257.
[8] S. Cavallaro, S. Freni, Int. J. Hydrogen Energy 21 (1996) 465.
[9] F.B. Noronha, M.C. Durão, M.S. Batista, L.G. Appel, Catal. Today 85 (2003) 13.
[10] I. Nowak, M. Ziolek, Chem. Rev. 99 (1999) 3603.
[11] K. Vasudeva, N. Mitra, P. Umasankar, S.C. Dhingra, Int. J. Hydrogen Energy 21 (1996) 13.
[12] X.-Y. Jiang, R.-X. Zhou, P. Pan, B. Zhu, X.-X. Yuan, X.-M. Zhen, Appl. Catal. A: Gen. 150 (1997) 131.
[13] J. Xiaoyuan, L. Liping, C. Yingxu, Z. Xiaoming, J. Mol. Catal. A: Chem. 197 (2003) 193.
[14] M. Mavrikakis, M.A. Barteau, J. Mol. Catal. A: Chem. 131 (1998) 135.
[15] A. Yee, S.J. Morrison, H. Idriss, J. Catal. 186 (2000) 279.
[16] A. Yee, S.J. Morrison, H. Idriss, J. Catal. 191 (2000) 30.